Details of each benchmark line

Sho Iwamoto

Details (fail safe note) for each of my analyses.

1 Prerequisites

1.1 Decay chain and accepted signal categorization

We use the following notation for (s)leptons to avoid confusion in this note (but possibly be avoided in the paper).

$$\tilde{l}_{\rm L} = (\tilde{e}_{\rm L}, \tilde{\mu}_{\rm L}, \tilde{\tau}_{\rm L}), \qquad \tilde{\nu} = (\tilde{\nu}_e, \tilde{\nu}_\mu, \tilde{\nu}_\tau), \qquad \text{slepton} = (\tilde{l}_{\rm L}, \tilde{\nu}, (\tilde{l}_{\rm R})),$$
$$l = (e, \mu, \tau), \qquad \ell = (e, \mu), \ldots$$

In addition, to reinterpret LHC analyses, we use the following labels for simplified models ("chain"s):

$$\text{NC/3L} : \tilde{\chi}^0\tilde{\chi}^\pm \to \left[\left(\tilde{l}_{\rm L}^{(*)} l^{(*)}, \tilde{\nu}^{(*)}\tilde{\nu}^{(*)}; 1/12 \text{ each}\right)\left(\tilde{\nu} l, \tilde{l}_{\rm L}\nu; 1/6 \text{ each}\right)\right] \otimes (\text{slep} \to \text{lep}\tilde{\chi}^0_{\rm LSP}; 100\%) \tag{1.1}$$
$$\text{NC/LLT} : \tilde{\chi}^0\tilde{\chi}^\pm \to \left[\left(\tilde{l}_{\rm R}^{(*)} l^{(*)}; 1/6 \text{ each}\right)\left(\tilde{\tau}_{\rm R}\nu; 100\%\right)\right] \otimes (\text{slep} \to \text{lep}\tilde{\chi}^0_{\rm LSP}; 100\%) \tag{1.2}$$
$$\text{NC/WZ} : \tilde{\chi}^0\tilde{\chi}^\pm \to (Z\tilde{\chi}^0_{\rm LSP})(W^\pm\tilde{\chi}^0_{\rm LSP}) \ \text{(possibly virtual)}, \tag{1.3}$$
$$\text{NC/WH} : \tilde{\chi}^0\tilde{\chi}^\pm \to (H\tilde{\chi}^0_{\rm LSP})(W^\pm\tilde{\chi}^0_{\rm LSP}) \ \text{(possibly virtual)}, \tag{1.4}$$
$$\text{CC/2L} : \tilde{\chi}^+\tilde{\chi}^- \to \left[\left(\tilde{\nu} l^*, \tilde{l}_{\rm L}^* \nu; 1/6 \text{ each}\right)\left(\tilde{\nu}^* l, \tilde{l}_{\rm L}\nu^*; 1/6 \text{ each}\right)\right] \otimes (\text{slep} \to \text{lep}\tilde{\chi}^0_{\rm LSP}; 100\%), \tag{1.5}$$
$$\text{SLSL} : (\tilde{l}_{\rm L}\tilde{l}_{\rm L}^* \text{ or } \tilde{l}_{\rm R}\tilde{l}_{\rm R}^*; 6 \text{ particles degen.}) \otimes (\text{slep} \to \text{lep}\tilde{\chi}^0_{\rm LSP}; 100\%), \tag{1.6}$$

where the virtual Z, $W^\pm$, and H are assumed to decay according to the SM theoretical branching ratio.

1.2 Our approximation

In SUSY searches by the ATLAS and CMS collaborations, they represent the results in several ways. The 95% confidence upper limit on production cross section, $\sigma_{\rm UL}$, is one of such forms, where a simplified SUSY scenario and particular production processes are considered and consistency with the Standard Model is given by the upper limit on the production cross section of the particular processes. A model is excluded with 95% confidence level if $\sigma_{\rm UL}$ is smaller than the theoretical cross section $\sigma_{\rm theory}$.

If $\sigma_{\rm UL}$ is calculated from one signal region (SR), it is related to the upper limit on the number of events in the SR, $N_{\rm UL}$, by

$$\frac{N_{\rm UL}}{\mathcal{L}} = (\mathcal{A}\cdot\mathcal{E})\cdot\sigma_{\rm UL;original}. \tag{1.7}$$

Here, we introduce a label "original" to clarify that the limit is for their original simplified scenario. The left-hand side is independent of the processes or models, where $\mathcal{L}$ is the integrated luminosity, while the process dependence is contained in the acceptance $\mathcal{A}$ and efficiency $\mathcal{E}$. Therefore, their result can be applied to any models X if we calculate the acceptance and efficiency for the model X; specifically, we should compare $\sigma_{X;\rm theory}$ with

$$\sigma_{{\rm UL};X} := \frac{(\mathcal{A}\cdot\mathcal{E})_{\rm original}}{(\mathcal{A}\cdot\mathcal{E})_X}\cdot\sigma_{\rm UL;original}. \tag{1.8}$$

$(\mathcal{A}\cdot\mathcal{E})_X$ however requires Monte Carlo simulation with full detector simulation. To avoid such complexity, we approximate the ratio by, assuming that X is similar to the original process,

$$\frac{(\mathcal{A}\cdot\mathcal{E})_{\rm original}}{(\mathcal{A}\cdot\mathcal{E})_X} \approx \frac{A_{\rm original}}{A_X} =: \frac{1}{K_\Gamma}, \tag{1.9}$$

where A, simplified acceptance, is calculated just from the decay ratios of the relevant particles.

The above procedure is less justifiable if $\sigma_{\mathrm{UL;original}}$ is given by statistical combination of multiple SRs[*1], but we will apply it as far as the expression of A is common for, or at worst, the values of K_Γ are similar for, the SRs combined.

Then, this upper limit is compared with the theoretical production cross section σ_X:

$$\sigma_X \quad \text{v.s.} \quad \sigma_{\mathrm{UL};X} = \frac{A_{\mathrm{original}}}{A_X}\sigma_{\mathrm{UL;original}}. \tag{1.10}$$

Note that these variables have physical sense. There is an equivalent comparison,

$$A_X\sigma_X \quad \text{v.s.} \quad A_{\mathrm{original}}\sigma_{\mathrm{UL;original}}, \tag{1.11}$$

which may be useful in some cases because the model dependence is contained in one side.

2 LHC Analyses

2.1 ATLAS 1803

ATLAS 1803 [**?**] has the following analyses[*2]:

(a) CC/2L(0.5) — $(2\ell)_{\mathrm{OS}}0j$ — Fig. 8(a) — `10.17182/hepdata.81996.v1/t78`

(b) SLSL — $(2\ell)_{\mathrm{OS}}0j$ — Fig. 8(b) — `10.17182/hepdata.81996.v1/t79`

(c) NC/3L(0.5) — $(3\ell)_{\mathrm{SFOS}}$ — Fig. 8(c) — `10.17182/hepdata.81996.v1/t80`

(d) NC/WZ — $(3\ell)_{\mathrm{SFOS}} \oplus (2\ell)_{\mathrm{SFOS}}2j$ — Fig. 8(c) — `10.17182/hepdata.81996.v1/t81`,

where the first (second) column shows the considered chains (signal regions for the analysis), the third column gives the references to the exclusion plot on the paper, and the last column shows the DOIs to the data resources of σ_{UL}.

Since our scenarios with $x = 0.50$ is similar to the model NC/3L(0.5), reinterpretation of their analysis (c) will give an estimation of LHC bounds to them. Noting the requirement of SFOS pair, the probability that chain-NC/3L with $x = 0.5$ produces signatures falling in the category is estimated by

$$p\Big((3\ell)_{\mathrm{SFOS}}\Big|\mathrm{NC/3L(0.5)}\Big) \approx \left[p(\tilde{\ell},\tilde{\nu}_\ell|\tilde{\chi}_1^\pm) + p_\ell \cdot p(\tilde{\tau},\tilde{\nu}_\tau|\tilde{\chi}_1^\pm)\right]\left[p(\tilde{\ell}^{(*)}|\tilde{\chi}_2^0) + \frac{3p_\ell^2}{4}\cdot p(\tilde{\tau}^{(*)}|\tilde{\chi}_2^0)\right], \tag{2.1}$$

which we will use the simplified acceptance $A(\mathrm{ATLAS1803c})$. Here, $p_\ell \simeq 0.352$ is the leptonic decay rate of τ. Also note that, here and hereafter, $\mathrm{Br}(\mathrm{slep} \to \mathrm{lep} + \tilde{\chi}_1^0) = 1$ (as well as flavor conservation) is assumed.

We similarly obtain the expressions of A for the other analyses. The result is summarized as

$$A(\mathrm{ATLAS1803b}) = 1, \tag{2.2}$$

$$A(\mathrm{ATLAS1803c}) = \left[p(\tilde{\ell},\tilde{\nu}_\ell|\tilde{\chi}_1^\pm) + p_\ell \cdot p(\tilde{\tau},\tilde{\nu}_\tau|\tilde{\chi}_1^\pm)\right]\left[p(\tilde{\ell}^{(*)}|\tilde{\chi}_2^0) + \frac{3p_\ell^2}{4}\cdot p(\tilde{\tau}^{(*)}|\tilde{\chi}_2^0)\right], \tag{2.3}$$

$$A(\mathrm{ATLAS1803d}) = \mathrm{Br}(\tilde{\chi}_1^\pm \to W^\pm\tilde{\chi}_1^0)\,\mathrm{Br}(\tilde{\chi}_2^0 \to Z\tilde{\chi}_1^0). \tag{2.4}$$

Here one should note that, though σ_{UL} for (d) is calculated by statistical combination of two very different signal categories, the expression of A is common for those two categories and hence we will use it. Also,

$$A(\mathrm{ATLAS1803b})_{\mathrm{original}} = 1, \tag{2.5}$$

$$A(\mathrm{ATLAS1803c})_{\mathrm{original}} = \left(\frac{4}{6} + \frac{2}{6}p_\ell\right)\left(\frac{4}{12} + \frac{3p_\ell^2}{4}\frac{2}{12}\right) = 0.273, \tag{2.6}$$

$$A(\mathrm{ATLAS1803d})_{\mathrm{original}} = 1. \tag{2.7}$$

[*1] Mainly because of the approximation $\mathcal{E}_{\mathrm{original}}/\mathcal{E}_X \approx 1$.

[*2] "SF", "OS", "SS" are respectively for same flavor, opposite sign, and same sign. $(3\ell)_{\mathrm{SFOS}}$ means that two of them form a SFOS pair and the other is arbitrary. Particles are "hard" (not soft) unless noted as such. Events with extra leptons are vetoed in some analyses, but I do not care those vetoes as we are anyway not interested in events to be vetoed.

2.2 CMS 1709

We use the following analyses in CMS1709 [**?**]:

(a) NC/3L(0.5) — $(3\ell)_{\rm SFOS}$ — Fig. 14

(b) NC/3L(0.05, 0.95) — $(3\ell)_{\rm SFOS} \oplus (2^{=}\ell)_{\rm SS}$ — Fig. 15a, 15b

(b1) NC/3L(0.05, 0.95) — $(2^{=}\ell)_{\rm SS}$ — Aux. Fig. 1, 3

(b2) NC/3L(0.05, 0.95) — $(3\ell)_{\rm SFOS}$ — Aux. Fig. 2, 4

(c) NC/LLT(0.05,0.5,0.95) — $(3\ell)_{\rm SFOS} \oplus (2\ell)_{\rm SFOS}1\tau$ — Fig. 16a, 16c, 16b

(c1) NC/LLT(0.05,0.5,0.95) — $(3\ell)_{\rm SFOS}$ — Aux. Fig. 7, 5, 9

(c2) NC/LLT(0.05,0.5,0.95) — $(2\ell)_{\rm SFOS}1\tau$ — Aux. Fig. 8, 6, 10

(d) NC/WZ — $(3\ell)_{\rm SFOS}$ — Fig. 18a

(e) NC/WH — various signatures — Fig. 18b

The data are provided in `.root` format at `http://cms-results.web.cern.ch/cms-results/public-results/publications/SUS-16-039/`. Note that we use (b1), (b2), etc., whose data are provided in auxiliary plots, instead of (b) etc. because of the lack of reasonable A. We use, as the simplified acceptances,

$$A(\text{CMS1709a}) = A(\text{ATLAS1803c}), \quad \langle 0.273 \rangle \tag{2.8}$$

$$A(\text{CMS1709b2}) = A(\text{ATLAS1803c}), \quad \langle 0.273 \rangle \tag{2.9}$$

$$A(\text{CMS1709c1}) = A(\text{ATLAS1803c}), \quad \langle 0.246 \rangle \tag{2.10}$$

$$\begin{aligned} A(\text{CMS1709c2}) = {} & \frac{p_{\rm h} p_\ell^2}{2} p(\tilde{\tau}^{(*)}, \tilde{\nu}_\tau^{(*)} | \tilde{\chi}_1^\pm) p(\tilde{\tau}^{(*)} | \tilde{\chi}_2^0) + p_{\rm h} p(\tilde{\tau}^{(*)}, \tilde{\nu}_\tau^{(*)} | \tilde{\chi}_1^\pm) p(\tilde{\ell}^{(*)} | \tilde{\chi}_2^0) \\ & + \frac{p_{\rm h} p_\ell}{2} p(\tilde{\ell}^{(*)}, \tilde{\nu}_\ell^{(*)} | \tilde{\chi}_1^\pm) p(\tilde{\tau}^{(*)} | \tilde{\chi}_2^0), \quad \langle 0.445 \rangle \end{aligned} \tag{2.11}$$

$$A(\text{CMS1709d}) = A(\text{ATLAS1803d}), \quad \langle 1 \rangle \tag{2.12}$$

$$A(\text{CMS1709e}) = \text{Br}(\tilde{\chi}_1^\pm \to W^\pm \tilde{\chi}_1^0)\, \text{Br}(\tilde{\chi}_2^0 \to H \tilde{\chi}_1^0), \quad \langle 1 \rangle \tag{2.13}$$

where the values in $\langle \cdot \rangle$ is the original values.

3 Validation

As shown in Eq. (1.7), $\mathcal{A}\mathcal{E}\sigma_{\rm UL}$ is unique for each SR and independent of hypothesized models. If an SR is used in multiple analyses, we can check the validity of our approximation, Eq. (1.9), by comparing $A\sigma_{\rm UL}$ among the analyses.

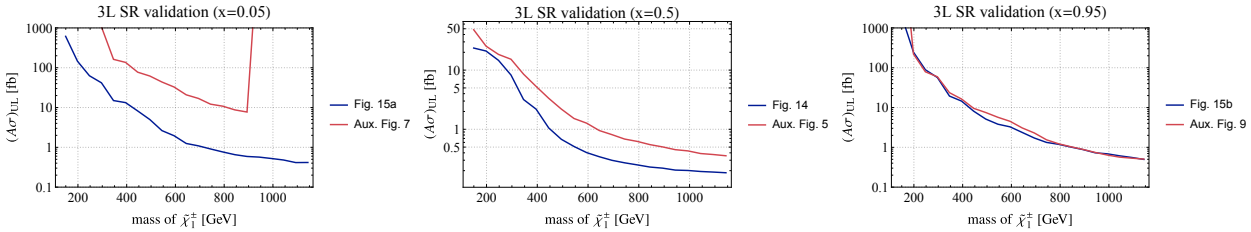

Figure 1: Comparison of $A\sigma_{\rm UL}$ for CMS 1709 $(3\ell)_{\rm SFOS}$ analyses. Dark-blue lines are of (a) and (b2) analyses for NC/3L chain, for which $A = 0.273$. Red ones are of (c1) for NC/LLT chain, for which $A = 0.246$.

3.1 ATLAS1803

This method does not provide validations for ATLAS 1803 results.

3.2 CMS1709

We can perform the validation for $(3\ell)_{\rm SFOS}$ analysis (the SR"3LA" in the original paper) by comparing (a) or (b2) with (c1). The results are shown in Fig. 1. Discrepancies are found in $x = 0.05$ and $x = 0.5$ cases.

The discrepancy in $x = 0.5$ case is probably due to the momentum difference of ℓ:

$$p_{\rm T}(3{\rm L}) \sim 0.5 \cdot \Delta m(\tilde{\chi}_1^\pm, \tilde{\chi}_1^0) \sim 0.25\tilde{\chi}_1^\pm, \qquad p_{\rm T}(3{\rm L}) \sim \frac{0.5}{3} \cdot \Delta m(\tilde{\chi}_1^\pm, \tilde{\chi}_1^0) \sim 0.083\tilde{\chi}_1^\pm. \tag{3.1}$$

While the $p_{\rm T}$ threshold is 10–25 GeV, this may give a factor 2–3 difference.

A worse discrepancy is observed in $x = 0.05$ case, which is probably caused by the CMS hypothesized model: they assume ${\rm Br}(\tilde{\chi}_1^\pm \to \tilde{\tau}^\pm \nu^{(*)}) = 1$ in the LLT case, while in 3L case (as well as our model points) ${\rm Br}(\tilde{\chi}_1^\pm \to \tilde{\tau}^\pm \nu^{(*)}) \sim {\rm Br}(\tilde{\chi}_1^\pm \to \tilde{\nu}^{(*)} \tau^\pm)$. The same argument works for $x = 0.95$; the resemblance in the plot is just by accident.

4 Line-by-line analysis

4.1 tab1-0.50

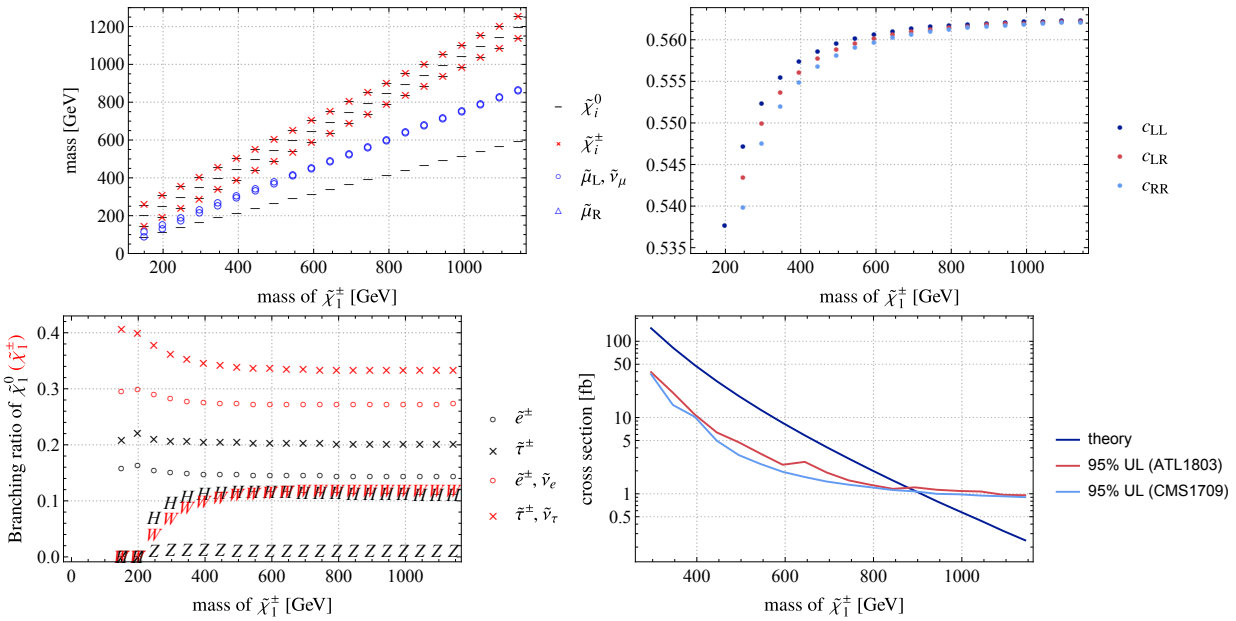

Figure 2: The property of tab1-0.50 benchmark line. The models are generated with $M_2 = 200, 250, \ldots, 1200\,\text{GeV}$, while $m_{\tilde{\chi}_1^\pm}$ is used as labels.
(A) Masses of relevant SUSY particles. Note that $\tilde{\mu}_R$ is decoupled.
(B) The cross-section c-factor (see `analysis.pdf`).
(C) The BRs of $\tilde{\chi}_1^\pm$ (red) and $\tilde{\chi}_2^0$ (black). The bottom black points are "H" and "Z" overlapped.
(D) The theoretical cross section and interpreted upper limits on it.

This line is characterized by

$$M_2 = \mu = 2M_1, \quad x = \frac{m_{\tilde{l}_L} - m_{\tilde{\chi}_1^0}}{m_{\tilde{\chi}_2^0} - m_{\tilde{\chi}_1^0}} = 0.5, \quad \tan\beta = 40, \quad \tilde{l}_R, \tilde{q}, \text{heavy-Higgs: decoupled.} \tag{4.1}$$

The mass spectrum is shown in Fig. 2; we use $m_{\tilde{\chi}_1^\pm}$ to label each model point. For $m_{\tilde{\chi}_1^\pm} > 300\,\text{GeV}$, the LSP is $\tilde{\chi}_1^0$ and $\tilde{\chi}_{2,3,4}^0 \tilde{\chi}_{1,2}^\pm$ may give NC/3L-chain. Meanwhile, we do not consider points with $m_{\tilde{\chi}_1^\pm} < 300\,\text{GeV}$ as neither by ATLAS. We safely ignore $\tilde{\chi}_3^0$ because of non-degeneracy and smaller production rate, as it has less $\tilde{W}$-component. A degenerate pair $\tilde{\chi}_4^0 \tilde{\chi}_2^\pm$ may serve as the chain-3L target, but since we have no way to include its contribution, we ignore it, which has a smaller production rate. Hence, we consider only the NC/3L chain produced by $pp \to \tilde{\chi}_2^0 \tilde{\chi}_1^\pm$.

The cross section is, since the c-factors are similar for $m_{\tilde{\chi}_1^\pm} > 300\,\text{GeV}$, given by

$$\sigma(pp \to \tilde{\chi}_2^0 \tilde{\chi}_1^\pm) \approx K_\sigma \cdot \sigma(pp \to \tilde{W}^\pm \tilde{W}^3); \qquad K_\sigma = \text{mean}(c_{LL}, c_{LR}, c_{RR}), \tag{4.2}$$

where the pure-wino production cross section $\sigma(pp \to \tilde{W}^\pm \tilde{W}^3)$ is taken from LHCSUSYXSWG[*3].

The results against ATLAS1803 is shown in **??**, where the black dots correspond to $K_\sigma K_\Gamma \sigma(\text{Wino})$. It shows that the ATLAS1803 analysis nearly excludes below $\sim 860\,\text{GeV}$. The wiggles in σ_{UL} is due to interpolation of the σ_{UL}-grid ATLAS provides, for which logarithmic interpolation (i.e., linear interpolation on the function $\log \sigma_{UL}(m_{\tilde{\chi}_1^\pm}, m_{\tilde{\chi}_1^0})$) is used.

We may discuss the validity of our approximation consulting Fig. 1 for $x = 0.5$, where our σ_{UL} may be aggressive by factor 2 at worst. It is however too pessimistic, as the electroweakino decay branch are approximately flavor-democratic. As $\text{Br}(\tilde{\chi}_1^\pm \to \tilde{\tau}^\pm)/\text{Br}(\tilde{\chi}_1^\pm \to \tilde{e}^\pm) \sim 1.3$, 30% uncertainty will be enough in this case.

[*3] `https://twiki.cern.ch/twiki/bin/view/LHCPhysics/SUSYCrossSections13TeVn2x1wino`

4.2 tab1-0.05

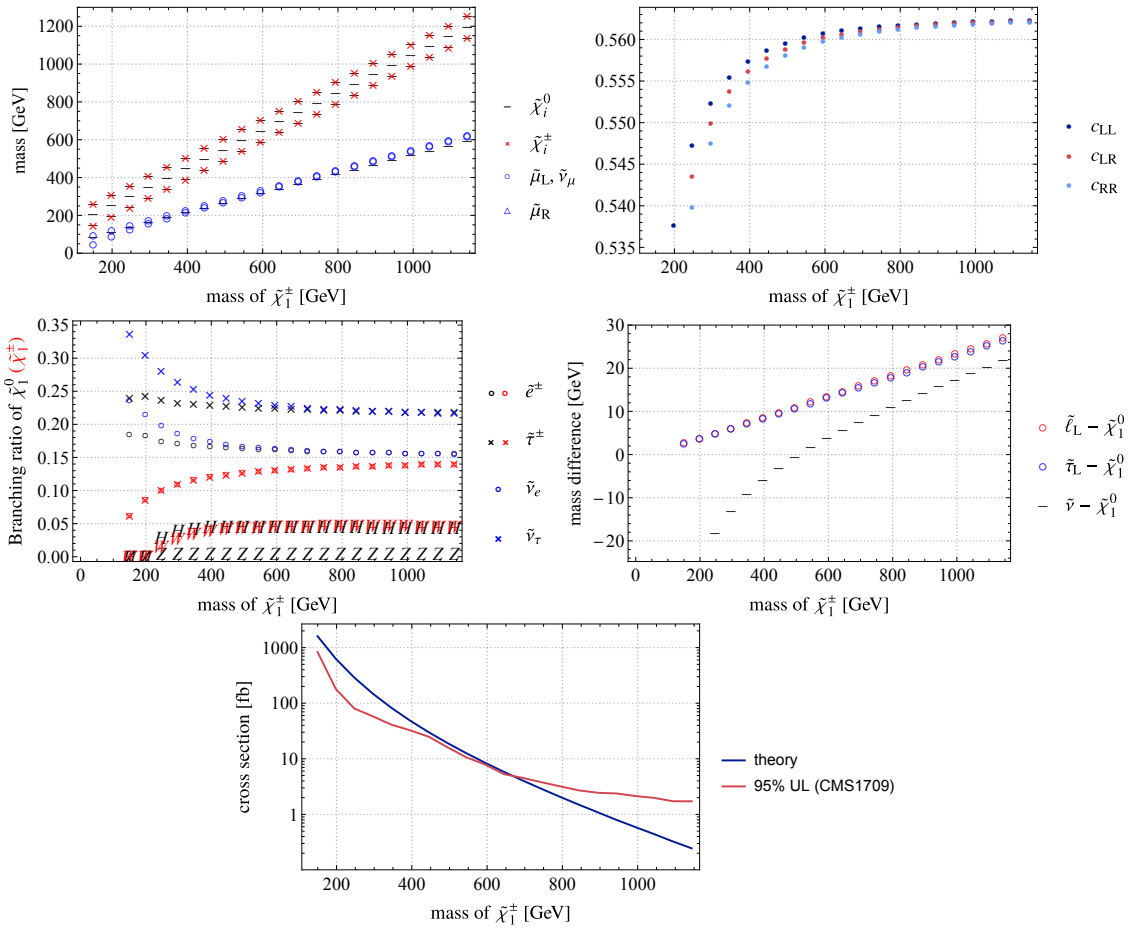

Figure 3: The property of tab1-0.50 benchmark line. The models are generated with $M_2 = 200, 250, \ldots, 1200\,\mathrm{GeV}$, while $m_{\tilde{\chi}_1^\pm}$ is used as labels.
(A) Masses of relevant SUSY particles. Note that $\tilde{\mu}_R$ is decoupled.
(B) The cross-section c-factor (see `analysis.pdf`).
(C) The BRs of $\tilde{\chi}_1^\pm$ (red/blue) and $\tilde{\chi}_2^0$ (black). See text for details since this plot is too complicated.
(D) The mass differences between SUSY particles. The LSP is $\tilde{\nu}$ for $m_{\tilde{\chi}_1^\pm} \lesssim 500\,\mathrm{GeV}$.
(E) The theoretical cross section and interpreted upper limits on it.

As in the previous case, we focus on $\tilde{\chi}_2^0\tilde{\chi}_1^\pm$ production and calculate the cross section. The LSP is $\tilde{\chi}_1^0$ ($\tilde{\nu}$) for $m_{\tilde{\chi}_1^\pm} \gtrsim 500\,\mathrm{GeV}$ ($\lesssim 500\,\mathrm{GeV}$). At the collider, however, the LSP does not matter much because $\tilde{l}^\pm$ mainly decays to $\tilde{\chi}_1^0$ and it is invisible even if it is not the LSP. One may claim that the $\tilde{\nu}$-LSP will, or actually the mass between $\tilde{l}^\pm$ and $\tilde{\nu}$, which is not included in the LHC analyses, will, increase $\mathcal{A}\cdot\mathcal{E}$ because the resulting ℓ will have larger p_T.

Figure 3 (C) shows the branching ratios of $\tilde{\chi}_2^0$ and $\tilde{\chi}_1^\pm$. Focusing on the black points, we see $\tilde{\chi}_2^0$ slightly prefer $\tilde{\tau}\tau$ to $\tilde{\ell}\ell$. Meanwhile, $\tilde{\chi}_1^\pm$ (non-black points) prefers $\tilde{\nu}_\tau\tau$ to $\tilde{\nu}_\ell\ell$ but the ratios to charged sleptons are flavor-universal. dd .These observations are critical if we discuss the validity of our approximation. Our models are again very different from "LLT chain" (Aux. Fig. 7), and thus the uncertainty estimation in $x = 0.5$ case is valid here.

The resulting bound is $m_{\tilde{\chi}_1^\pm} > 650\,\mathrm{GeV}$ but considering the uncertainty we should claim that the bound should be somewhere between 400–650 GeV.

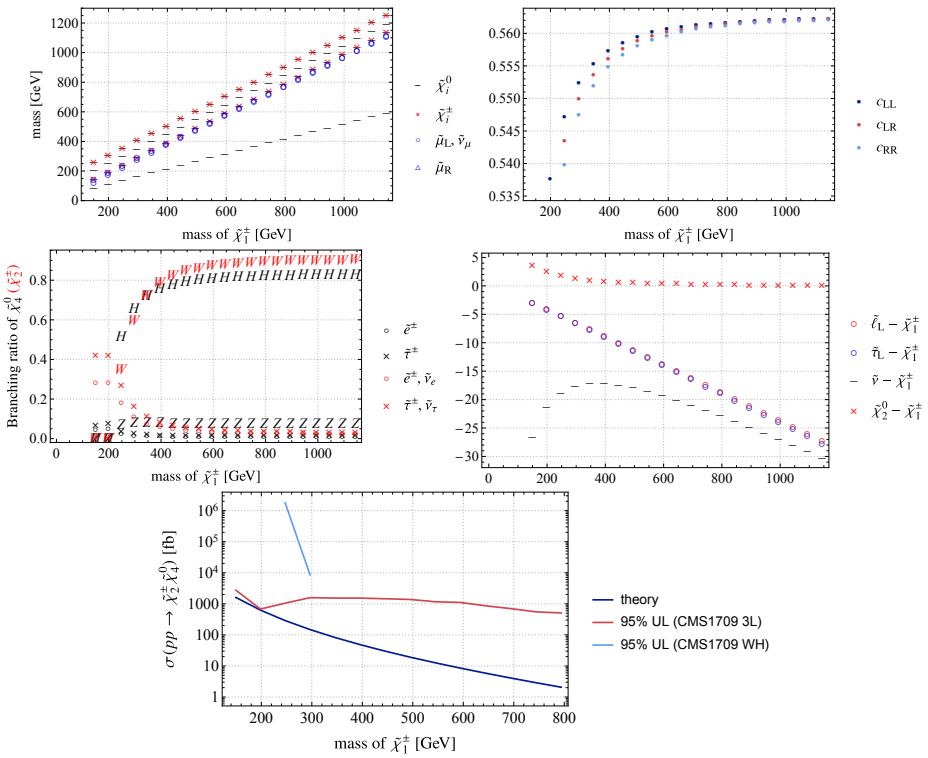

Figure 4: The property of tab1-0.95 benchmark line. The models are generated with $M_2 = 200, 250, \ldots, 1200\,\text{GeV}$, while $m_{\tilde{\chi}_1^\pm}$ is used as labels.
(A) Masses of relevant SUSY particles. Note that $\tilde{\mu}_R$ is decoupled. (B) The cross-section c-factor (see `analysis.pdf`). (C) The BRs of $\tilde{\chi}_1^\pm$ (red) and $\tilde{\chi}_2^0$ (black).
(D) The mass differences between SUSY particles. The LSP is $\tilde{\nu}$ for $m_{\tilde{\chi}_1^\pm} \lesssim 500\,\text{GeV}$.
(E) The theoretical cross section of $pp \to \tilde{\chi}_1^\pm \tilde{\chi}_2^0$ and interpreted upper limits on it.

4.3 tab1-0.95

On this line, $\tilde{\chi}_2^0$ has very small BRs to $\tilde{\ell}$ or Z; because of the phase space suppression, it mainly decays to $H\tilde{\chi}_1^0$ for $m_{\tilde{\chi}_1^\pm} \gtrsim 250\,\text{GeV}$ and to $\tilde{\nu}\nu$ for $m_{[\tilde{\chi}_1^\pm]} \lesssim 250\,\text{GeV}$. Therefore, CMS1709 (b) and (c) does not give any limits as far as we consider $\tilde{\chi}_2^0\tilde{\chi}_1^\pm$ production. Meanwhile, the search for $WH + \not{E}_T$, i.e., (e) gives very weak constraints. So we cannot constrain the models on this line in this study.

In actual experiments, the models should be covered by CMS1709 (b) and (c) because of the events from $pp \to \tilde{\chi}_4^0\tilde{\chi}_2^\pm$. Our study cannot cover this process because they have smaller x; it requires MC simulation. However, assuming that x closer to 0.5 should give better $\mathcal{A} \times \mathcal{E}$, we can give a conservative upper limit on $\sigma(pp \to \tilde{\chi}_4^0\tilde{\chi}_2^\pm)$ with using the CMS upper limits for $x = 0.95$. The result is shown in **??**; K_Γ and K_σ for $\tilde{\chi}_4^0\tilde{\chi}_2^\pm$ are prepared, and $\sigma_{\text{CMS1709a};x=0.95}$ is used (and hence the limit is very conservative). Accordingly, the lower bound of 150–200 GeV on $m_{\tilde{\chi}_1^\pm}$ is observed.

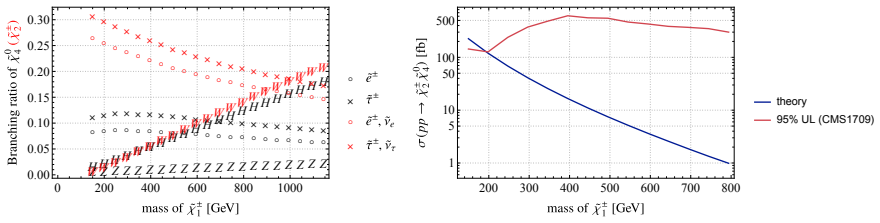

Figure 5: The extra property of tab1-0.50 benchmark line. (A) The BRs of $\tilde{\chi}_2^\pm$ (red) and $\tilde{\chi}_4^0$ (black). (B) The theoretical cross section of $pp \to \tilde{\chi}_2^\pm \tilde{\chi}_4^0$ and interpreted upper limits on it.

References